Electronic Supplementary Material (ESI) for ChemComm.

Selective and Benign Alkylation of Sulfido-Oxo Stannate Clusters with Propyl, Pentyl, or Hexyl Substituents

Gina Stuhrmann,[a] Jannik Schneider,[b] Kilian Schmidt,[b] and Stefanie Dehnen*[a]

[a] *Institute of Nanotechnology, Karlsruhe Institute of Technology, P.O. Box 3640, 76021 Karlsruhe, Germany*

[b] *Fachbereich Chemie und Wissenschaftliches Zentrum für Materialwissenschaften (WZMW), Philipps-Universität Marburg, Hans-Meerwein-Str. 4, 35043 Marburg, Germany*

SUPPORTING INFORMATION

1. Methods

1.1 General Synthesis Methods

All reactions (except the syntheses of the ionic liquids) and measurements were carried out under strong exclusion of oxygen and moisture, in a dry argon atmosphere using standard Schlenk technique or a glovebox (type Unilab plus; MBraun). The starting material $Na_4[SnS_4]\cdot 14H_2O$ was prepared by reacting $Na_2S\cdot 9H_2O$ and $SnCl_4\cdot 5H_2O$ according to the literature.[1] $Na_2S\cdot 9H_2O$ (Sigma-Aldrich, ≥98 %) and $SnCl_4\cdot 5H_2O$ (Sigma-Aldrich, 98 %) were used as received. Water was degassed by application of dynamic vacuum for 30 minutes (2 times). 2-Methylimidazole (Fisher Scientific GmbH, 99 %), 1-bromo-propane (Thermo Scientific Chemicals, 99 %), 1-bromo-pentane (Sigma-Aldrich, 98 %), 1-bromo-hexane (Sigma-Aldrich, 98 %) and NaH (Tokyo Chemical Industry Co., Ltd. 60 %, dispersion in Paraffin Liquid) were used for the synthesis of **A**, **i**, and **ii** as received. THF and pentane were purified by distillation. CH_3CN and CD_3CN were dried over calcium hydride, purified by distillation, and stored over 3 Å molecular sieve until use. An illustration of an ionothermal reaction ampoule is shown in Figure S1.

1.2 Synthesis of $(C_3C_1C_3Im)Br$ (A)

The ionic liquid **A** was prepared according to a literature method,[2] yet under air and in larger scale (50 g instead of 2 g).

1.3 Synthesis and crystallization of $(C_5C_1C_5Im)Br$ (i)

The synthesis of the new ionic liquid **i** was adopted from the literature method for the synthesis of $(C_3C_1C_3Im)Br$,[2] yet under air and in larger scale (50 g instead of 2 g). Crystals of **i** form instantly upon mixing a drop of immersion oil (NVH oil Cat. NVHO-1 from Jena Bioscience GmbH) with a drop of freshly synthesized **i**.

^{1}H-NMR (500.2 MHz, $CDCl_3$, 293 K): δ [ppm] = 7.56 (s, 2H, $C_{Im}H$); 4.26 (t, J = 7.3 Hz, 4H, CH_2); 2.81 (s, 3H, CH_3); 1.84 (m, 4H, CH_2); 1.34 (m, 8H, CH_2); 0.90 (t, 6H, J = 5.8 Hz, CH_3)

^{13}C-NMR (126 MHz, $CDCl_3$, 293 K) δ [ppm] = 143.26 (s, $C_{Im}Me$); 121.75 (s, C_{Im}); 49.23 (s, CH_2); 29.65 (s, CH_3); 28.55 (s, CH_2); 22.26 (s, CH_2); 13.94 (s, CH_2); 11.19 (s, CH_3)

1.4 Synthesis of $(C_6C_1C_6Im)Br$ (ii)

The synthesis of the new ionic liquid **ii** was adopted from the literature method for the synthesis of $(C_3C_1C_3Im)Br$,[2] yet under air and in larger scale (50 g instead of 2 g).

^{1}H-NMR (500.2 MHz, $CDCl_3$, 293 K): δ [ppm] = 7.55 (s, 2H, $C_{Im}H$); 4.25 (t, J = 7.4 Hz, 4H, CH_2); 2.81 (s, 3H, CH_3); 1.83 (m, 4H, CH_2); 1.31 (m, 12H, CH_2); 0.87 (t, 6H, J = 6.0 Hz, CH_3)

^{13}C-NMR (126 MHz, CD_3CN, 293 K) δ [ppm] = 143.27 (s, $C_{Im}Me$); 121.72 (s, C_{Im}); 49.26 (s, CH_2); 31.27 (s, CH_3); 29.91 (s, CH_2); 26.16 (s, CH_2); 22.51 (s, CH_2); 14.02 (s, CH_2), 11.21 (s, CH_3)

1.5 Synthesis of $(C_3C_1C_3Im)_4[Sn_{10}O_4S_{16}(SPr)_4]$ (1)

65 mg of $Na_4[SnS_4]\cdot 14H_2O$ (0.11 mmol, 1.0 eq.) and 500 mg of $(C_3C_1C_3Im)Br$ were weighed into a borosilicate glass ampoule, with a volumetric capacity of 7 mL. The ampoule was sealed under vacuum and heated in an oven (NABERTHERM) to 180 °C at an heating rate of 30 °C/h, kept at 150 °C for 72 h, and then cooled down to room temperature at a cooling rate of 5 °C/h. Colorless plates of **1** were obtained in approximately 34 % yield (based on Sn). The crude product was re-crystallized from CH_3CN to obtain better quality crystals (Figure S2).

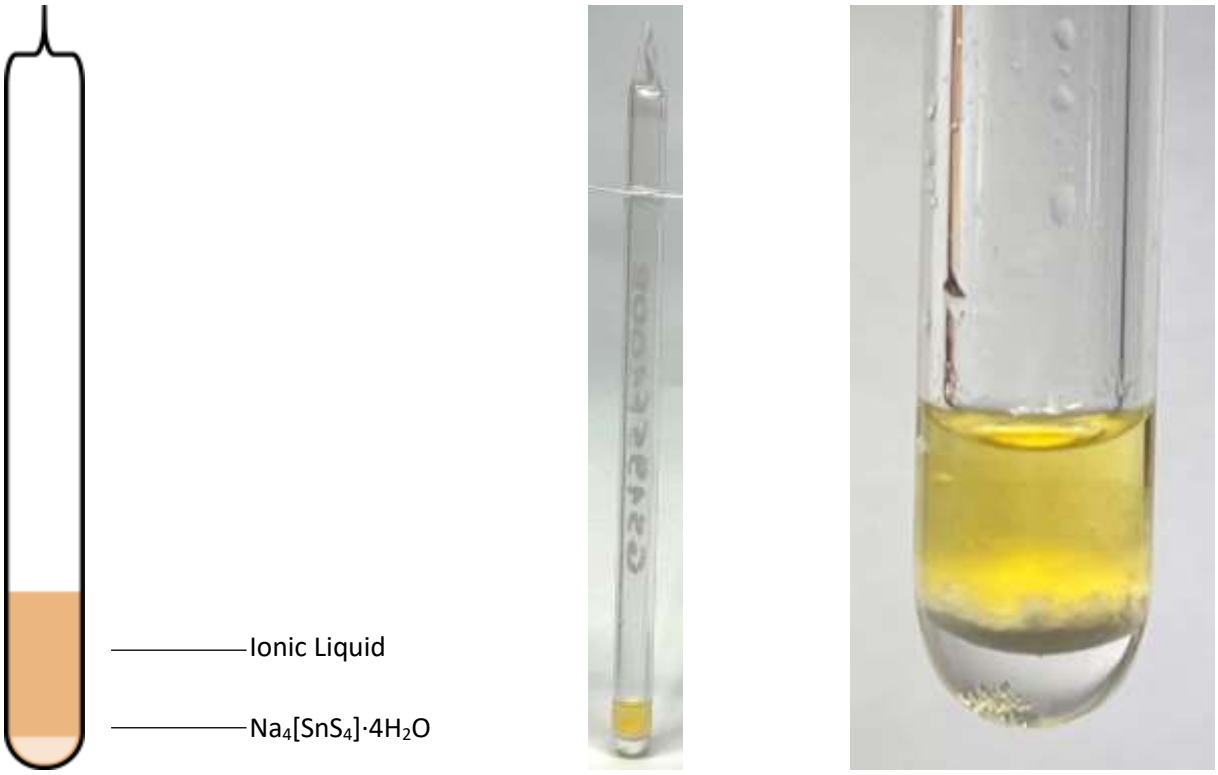

Figure S1. Schematic drawing of a sealed ampoule (left), photograph of an ampoule after being taken out of the oven (center) – with a zoom in into the part comprising the reaction products (right).

1.6 Synthesis of $(C_5C_1C_5Im)_4[Sn_{10}O_4S_{16}(SPn)_4]$ (2)

65 mg of $Na_4[SnS_4]\cdot 14H_2O$ (0.11 mmol, 1.0 eq.) and 500 mg of $(C_5C_1C_5Im)Br$ were weighed into a borosilicate glass ampoule, with a volumetric capacity of 7 mL. The ampoule was sealed under vacuum and heated in an oven (NABERTHERM) to 180 °C at an heating rate of 30 °C/h, kept at 150 °C for 72 h, and then cooled down to room temperature at a cooling rate of 5 °C/h. Colorless plates of **2** (Figure S2) were obtained in approximately 60 % yield (based on Sn).

1.7 Synthesis of $(C_6C_1C_6Im)_4[Sn_{10}O_4S_{16}(SHex)_4]$ (3)

65 mg of $Na_4[SnS_4]\cdot 14H_2O$ (0.11 mmol, 1.0 eq.) and 500 mg of $(C_6C_1C_6Im)Br$ were weighed into a borosilicate glass ampoule, with a volumetric capacity of 7 mL. The ampoule was sealed under vacuum and heated in an oven (NABERTHERM) to 180 °C at an heating rate of 30 °C/h, kept at 150 °C for 72 h, and then cooled down to room temperature at a cooling rate of 5 °C/h. Colorless plates of **3** (Figure S2) were obtained in approximately 62 % yield (based on Sn).

1.8 Light microscopy

Visual inspection of crystals of **1**, **2** and **3** (Figure S2) was performed with a stereo light microscope SteREO Discovery.V8 by Carl Zeiss. The microscope was equipped with a high-intensive cold-light source CL 1500 ECO, an Achromat S 0.63x objective (FWD 107 mm), a PL 10x/21 Br ocular, and an AxioCam MRc 5 camera with a 60N-C 2/3'' 0,63x adapter. The raw photo material was examined by the AxioVision40x64 4.9.1 SP1 software.

1.9 Micro-X Ray Fluorescence (XRF) Spectroscopy

μ-XRF data were recorded on a Bruker M4 Tornado, equipped with an Rh-target X-ray tube and a silicon drift detector. The emitted fluorescence photons were detected with an acquisition time of 240 s. Upon deconvolution of the spectra, quantification of the elements was achieved based on the S K, Br K and Sn L radiation. The spectra are shown in Figures S3, S4 and S5, Tables S1, S2 and S3 summarize the data that confirm the heavy-atom ratio of compounds **1**, **2** and **3**.

1.10 Single-Crystal X-ray Diffraction

Crystals suitable for X-ray diffraction analyses of compounds **i**, **1, 2** and **3** were investigated with a STOE StadiVari diffractometer at 100 K, using Cu-Kα radiation (λ = 1.54186) from an X-ray micro source with X-ray optics and a Pilatus 300K Si hybrid pixel array detector. Upon scaling with spherical absorption correction (STOE X-Area Lana), the structure solution was performed by dual space methods, followed by full-matrix-least-squares refinement against F^2, using SHELXT15, SHELXL15 and OLEX2 software.[3–5] Table S4 summarizes the crystallographic data for compound **i**, and Table S5 summarizes the crystallographic data for compounds **1**, **2** and **3**. The structure of compound **1** is illustrated in Figure 1, for supplementary crystal structure figures, see Figures S6 – S9.

1.11 Single-Crystal Raman Spectroscopy

Raman data were collected on an S&I MonoVista CRS+ device. The measurements were performed with a laser wavelength of 532 nm and a grating of 300 grooves mm^{-1}. The measurements had a duration of 6 s with 10 coadditions. The Raman spectra of **1**,**2** and **3** are shown in comparison with the spectra of $(C_4C_1C_1Im)_4[Sn_{10}O_4S_{16}(SMe)_4]$[6] and $(C_4C_1C_4Im)_7[Sn_{10}O_4S_{16}(SBu)_4]Br_3$[7] in Figure S10.

1.12 NMR Spectroscopy

NMR studies of a solution of single crystals of compound **1**, **2** and **3** in CH_3CN-d3 were carried out on a Bruker DPX AV 500 at room temperature. The raw data were examined by means of MestReNova 6.0. ^{119}Sn NMR are given in Figure S11, S14 and S17, ^{1}H NMR spectra are given in Figure S12, S15 and S18, ^{13}C NMR spectra are given in Figure S13, S16 and S19.

1.13 Electrospray Ionization Mass Spectrometry (ESI-MS)

Mass spectra were recorded on a fresh solution of single crystals of **1**, **2**, and **3** with attached reaction medium in CH_3CN on a Thermo Fisher Scientific Finnigan LTQ-FT hybride mass spectrometer equipped with a linear ion trap (LTQ) and a FT-ICR (FT). Figures S20, S22, and S24 show the overview spectra, Figures S21, S23 and S25 show the high-resolution mass peaks.

1.14 Optical Absorption Spectroscopy

Optical absorption properties of compounds **1**, **2**, and **3** were measured under inert conditions employing a Varian Cary 5000 UV/VIS/NIR spectrometer from Agilent, equipped with a Praying Mantis accessory for the solid-state samples. To determine the optical band gaps, the raw data was transformed from reflectance *R* to absorption according to the Kubelka-Munk function:

$$F(R) = \frac{k}{s} = \frac{(1 - R_\infty)^2}{2R_\infty}$$

where k is the Kubelka-Munk absorption coefficient, R_∞ is the diffuse reflection, and s is the Kubelka-Munk scattering coefficient. The data is illustrated as a Tauc plot, where $(F(R) \cdot h\nu)^{1/n}$ is plotted against the energy (eV). For a direct band gap, n equals ½, for an indirect band gap, n equals 2. Since the transition in the region of interest was far more pronounced when choosing n = ½, we concluded that all analyzed compounds feature an indirect band gap.[8–11] The corresponding graphs are shown in Figures S26 – S28.

1.15 Photoluminescence Spectroscopy

Excitation and emission spectra in solution were measured on a Varian Cary Eclipse fluorescence spectrometer from *Agilent* with a xenon flash lamp (Figure S29 and S30).

Quantum yield measurements were performed with the solid state samples on a PTI QuantaMaster™ 8075-22 fluorometer with each double excitation and emission monochromators (HORIBA Jobin Yvon GmbH). Emission was detected on a R928 photomultiplier (250–800 nm) (HORIBA Jobin Yvon GmbH). Spectra were corrected for the wavelength dependent response of the detector and the spectrometer.

The following instrumental settings were used for data acquisition. Emission: excitation slitwidth: 4 nm, emission slitwidth: 4 nm, stepsize 0.05 nm, integration time: 0.5 sec. Excitation: excitation slitwidth: 4 nm, emission slitwidth: 4 nm, stepsize 0.05 nm, integration time: 0.5 sec.

2. Light microscopy

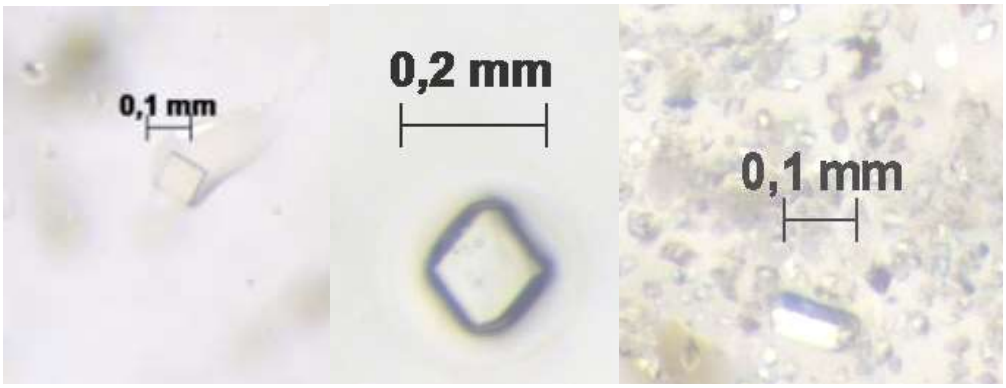

Figure S2. Light microscopy images of crystals of **1** (left), **2** (center), and **3** (right) in the ionic liquids.

3. Micro-X Ray Fluorescence (μ-XRF) Spectroscopy

Elemental analysis was carried out to investigate the heavy-atom ratio of the two compounds and exclude impurities. The bromine concentration can be explained with the residues of the ionic liquid on the surface of the crystals. The results are given in Tables S1 – S3, the spectra are shown in Figures S3 – S5.

3.1 μ-XRF of Compound 1

Table S1. Results of the μ-XRF analysis of compound **1**.

Element	X-Ray Series	Norm. Cont. (wt.%)	Atom Cont. (at.%)	Atom C. calc. (at.%)	Error (1
Sn	L series	66.51	35.63	33.30	0.11
S	K series	12.77	63.01	66.60	0.15
Br	K series	1.72	1.37	0	0.00

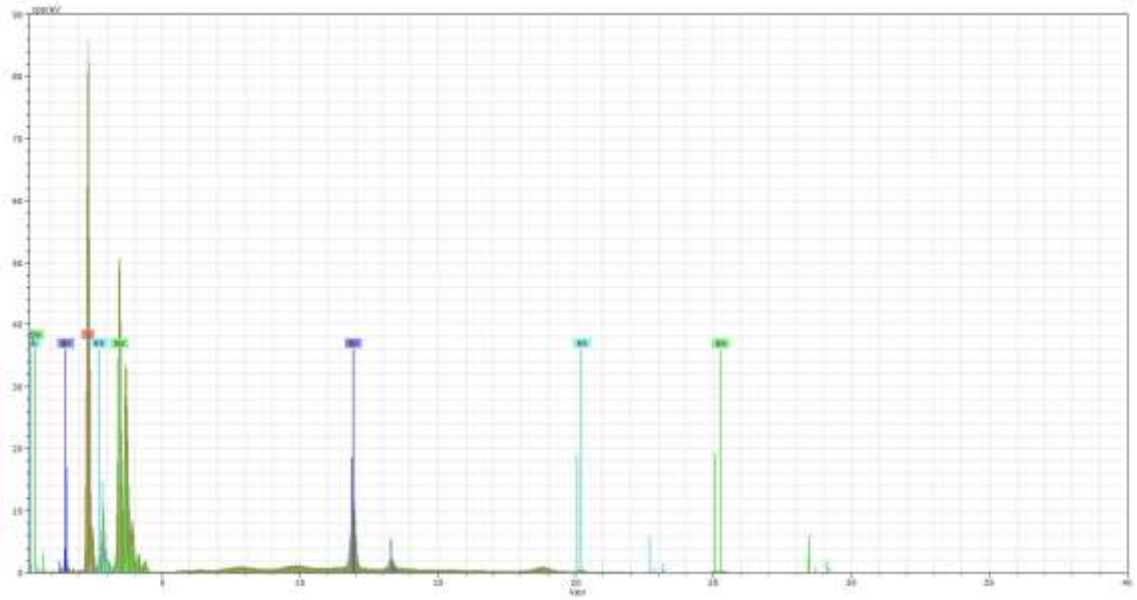

Figure S3. μ-XRF spectrum of compound **1**.

3.2 μ-XRF of Compound 2

Table S2. Results of the μ-XRF analysis of compound **2**.

Element	X-Ray Series	Norm. Cont. (wt.%)	Atom Cont. (at.%)	Atom C. calc. (at.%)	Error (1
Sn	L series	63.59	32.89	33.30	0.00
S	K series	34.14	65.37	66.60	0.00
Br	K series	2.26	1.74	0	0.00

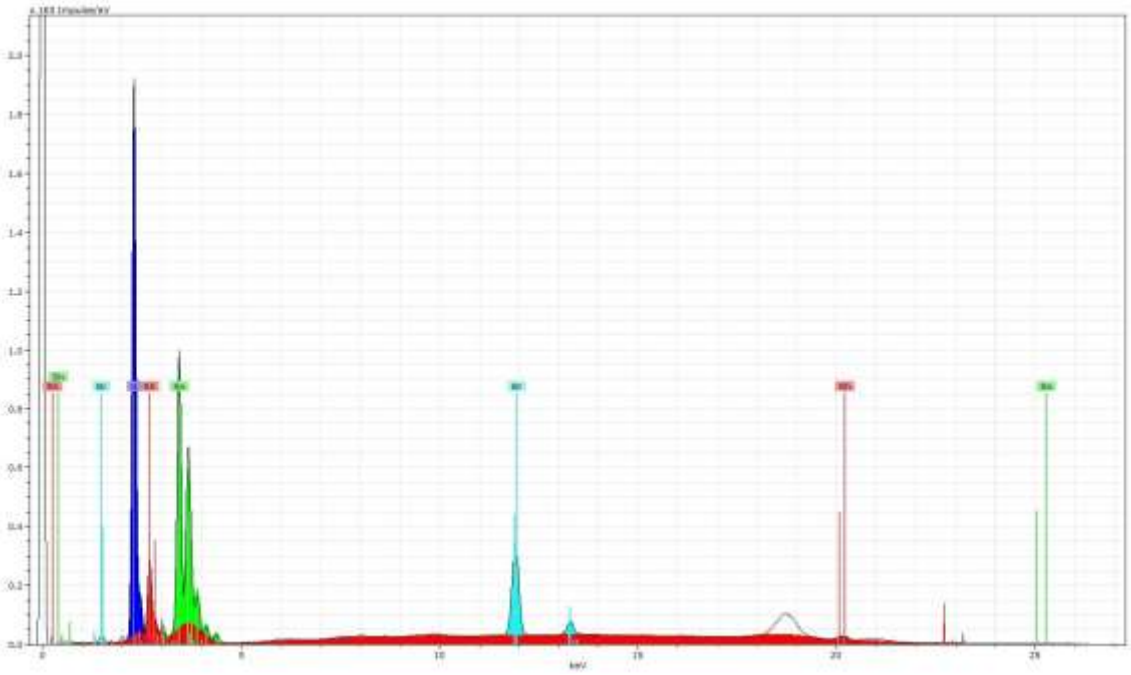

Figure S4. μ-XRF spectrum of compound **2**.

3.3 μ-XRF of Compound 3

Table S3. Results of the μ-XRF analysis of compound **3**.

Element	X-Ray Series	Norm. Cont. (wt.%)	Atom Cont. (at.%)	Atom C. calc. (at.%)	Error (1
Sn	L series	67.47	36.07	33.30	0.00
S	K series	32.53	63.93	66.60	0.00
Br	K series	0	0	0	0.00

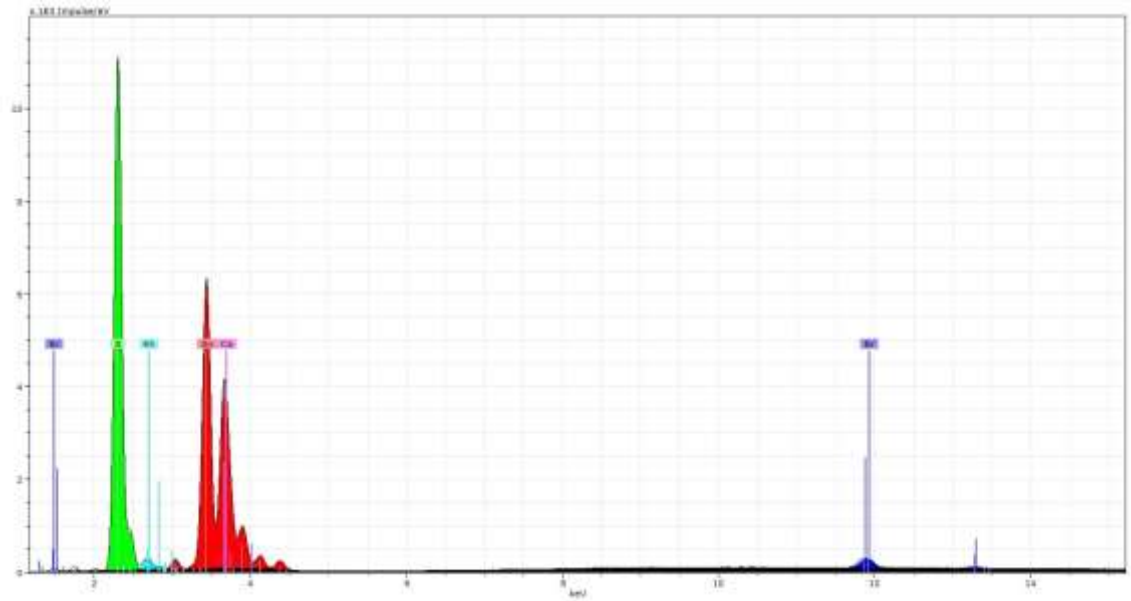

Figure S5. μ-XRF spectrum of compound **3**.

4. Single Crystal X-ray Diffraction (SC-XRD) Data

4.1 Crystallographic Data and Refinement Results

Table S4. Results of the SC-XRD analysis of compound **i**.

Compound (CCDC no.)	**i** (2281096)
Empirical formula	$C_{14}H_{27}N_2Br$
Chemical formula	$C_{14}H_{27}N_2Br$
Formula weight / g·mol^{-1}	303.28
Color & shape	Colorless needles
Crystal size / mm^3	0.23 × 0.18 × 0.11
Crystal system	Triclinic
Space group type	$P\bar{1}$
a / Å	8.8924(16)
b / Å	13.793(3)
c / Å	14.286(3)
α / °	113.979(13)
β / °	90.289(14)
γ / °	93.083(14)
V / Å^3	1597.9(5)
Z	4
ρ_{calc} / g·cm^{-3}	1.261
Radiation (*λ* /Å)	Cu-Kα (1.54186)
Temperature	100 K
μ / mm^{-1}	3.360
Min/max transmission	0.508/0.691
F(000)	640.0
θ range / °	7.518 – 152.526
No. measured refl.	31214
No. independent refl.	6503
No. indep. refl. ($I > 2\sigma(I)$)	4395
No. of parameters	313
No. of restraints	0
R(int)	0.0720
R_1 ($I > 2\sigma(I)$)	0.0602
wR_2 (all data)	0.1750
GooF (all data)	1.006
Hooft	–
S (all data)	1.006
Flack parameter	–
$\Delta\rho_{max}/\Delta\rho_{min}$ / e·Å^{-3}	0.85/–0.81

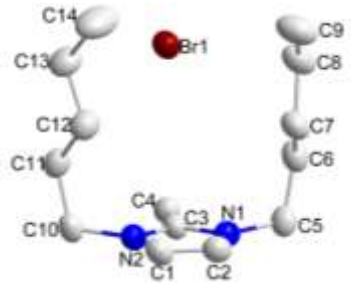

Figure S6. Asymmetric unit of the crystal structure of **i**. Hydrogen atoms are omitted for clarity; displacement ellipsoids are shown at the 50 % probability level. Color code: C grey, N blue, Br dark red.

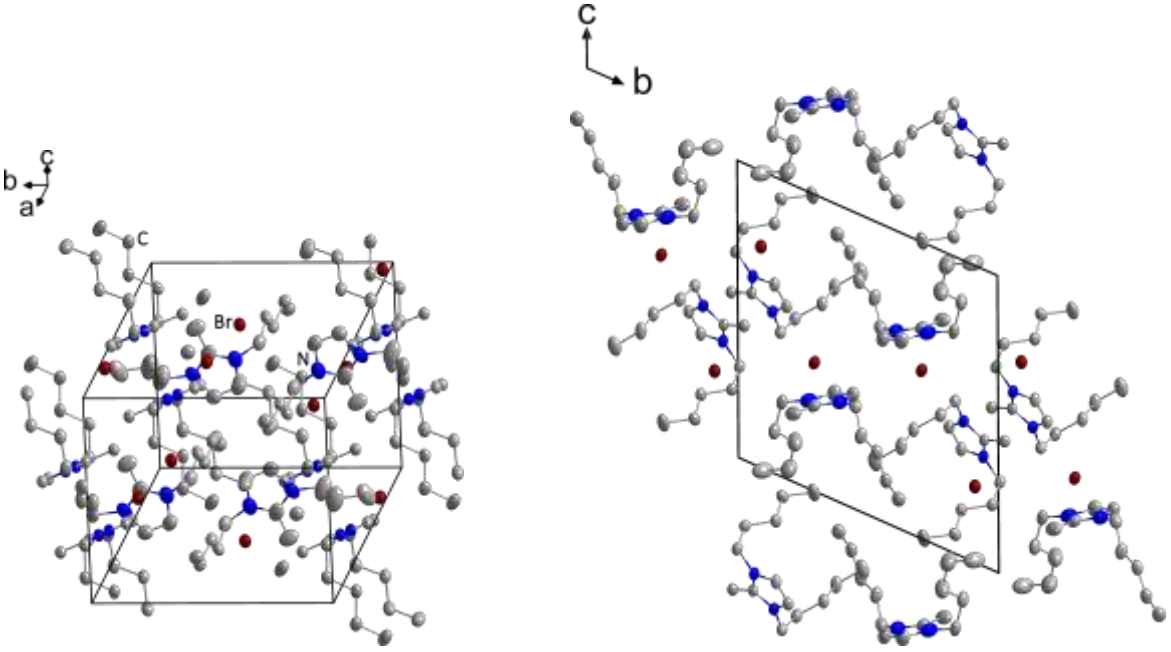

Figure S7. Cut-out of the crystal structure of **i** in two different views. H-atoms are omitted for clarity; displacement ellipsoids are shown at the 50 % probability level. Color code: C grey, N blue, Br dark red.

Compound **1**:

A solvent mask was applied, and 692 electrons were found in a volume of 2324 Å^3 in 1 void per unit cell. This is consistent with the presence of 1 pentane molecule per asymmetric unit, thus 4 pentane molecules (640 electrons) per unit cell (the pentane stemming from the thorough washing process before measuring them). Results of the SC-XRD analysis of compound **3** are summarized in Table S5.

Compound **2**:

A solvent mask was applied, and 297 electrons were found in a volume of 1972 Å^3 in 1 void per unit cell. This is consistent with the presence of 3 *n*-hexane molecules (150 electrons) per asymmetric unit, thus 6 *n*-hexane molecules (300 electrons) per unit cell (the *n*-hexane stemming from the thorough washing process before measuring them). Results of the SC-XRD analysis of compound **2** are summarized in Table S5. More details about intrinsic crystallographic problems are outlined below.

Compound **3**:

A solvent mask was applied, and 83 electrons were found in a volume of 1007 Å^3 in 1 void per unit cell. This is consistent with the presence of 1 pentane molecule per asymmetric unit, thus 2 pentane molecules (84 electrons) per unit cell (the pentane stemming from the thorough washing process before measuring them). Results of the SC-XRD analysis of compound **3** are summarized in Table S5. More details about intrinsic crystallographic problems are outlined below.

Table S5. Results of the SC-XRD analysis of compounds **1**, **2**, and **3**

Compound (CCDC no.)	**1** (2281097)	**2** (2281098)	**3** (2281099)
Empirical formula[1]	$C_{48}H_{84}N_8O_4S_{20}Sn_{10}$	$C_{49.67}H_{56.06}N_8O_4S_{20}Sn_{10}$	$C_{68.5}H_{97.34}N_8O_4S_{20}Sn_{10}$
Chemical formula[2]	$C_{68}H_{132}N_8O_4S_{20}Sn_{10}$	$C_{67.66}H_{98.06}N_8O_4S_{20}Sn_{10}$	$C_{73.5}H10_{9.33}N_8O_4S_{20}Sn_{10}$
Formula weight / g·mol^{-1}	2665.33	2668.98	2924.97
Color & shape	Colorless plates	Colorless plates	Colorless plates
Crystal size / mm^3	0.092 × 0.067 × 0.02	0.24 × 0.18 × 0.01	0.023 × 0.02 × 0.01
Crystal system	Tetragonal	Triclinic	Triclinic
Space group type	$I\bar{4}2d$	$P\bar{1}$	$P\bar{1}$
a / Å	19.9274(11)	19.5954(4)	18.7606(17)
b / Å	19.9274(11)	19.2861(5)	20.0088(19)
c / Å	26.2914(18)	19.7915(5)	21.1091(19)
α / °	90	99.744(2)	99.505(7)
β / °	90	112.258(2)	115.794(7)
γ / °	90	110.568(2)	110.290(7)
V / Å^3	10440.3(14)	6073.7(3)	6205.5(11)
Z	4	2	2
ρ_{calc} / g·cm^{-3}	1.696	1.459	1.565
Radiation (λ /Å)	Cu-Kα (1.54186)	Cu-Kα (1.54186)	Cu-Kα (1.54186)
Temperature	100 K	100 K	100 K
μ / mm^{-1}	22.695	19.512	19.152
Min/max transmission	0.425/0.990	0.0868/0.7942	0.3189/0.9123
F(000)	5120.0	2524.0	2833.0
θ range / °	5.564 to 152.496	5.586 to 135	5.646 to 153.212
No. measured refl.	102797	135107	125372
No. independent refl.	5441	21685	25303
No. indep. refl. ($I > 2\sigma(I)$)	4501	10202	13000
No. of parameters	210	741	902
No. of restraints	49	233	68
R(int)	0.0673	0.0604	0.0539
R_1 ($I > 2\sigma(I)$)	0.0371	0.0524	0.0456
wR_2 (all data)	0.0944	0.1632	0.1346
GooF (all data)	0.936	0.824	0.842
Hooft	0.016(5)	–	–
S (all data)	0.929	0.823	0.842
Flack parameter	0.031(6)	–	–
$\Delta\rho_{max}/\Delta\rho_{min}$ / e·Å^{-3}	0.51/–0.95	0.81/–0.86	0.96/–0.80

[1] Empirical formula excluding the solvent molecules calculated using the solvent mask.
[2] Chemical formula including the solvent molecules calculated using the solvent mask.

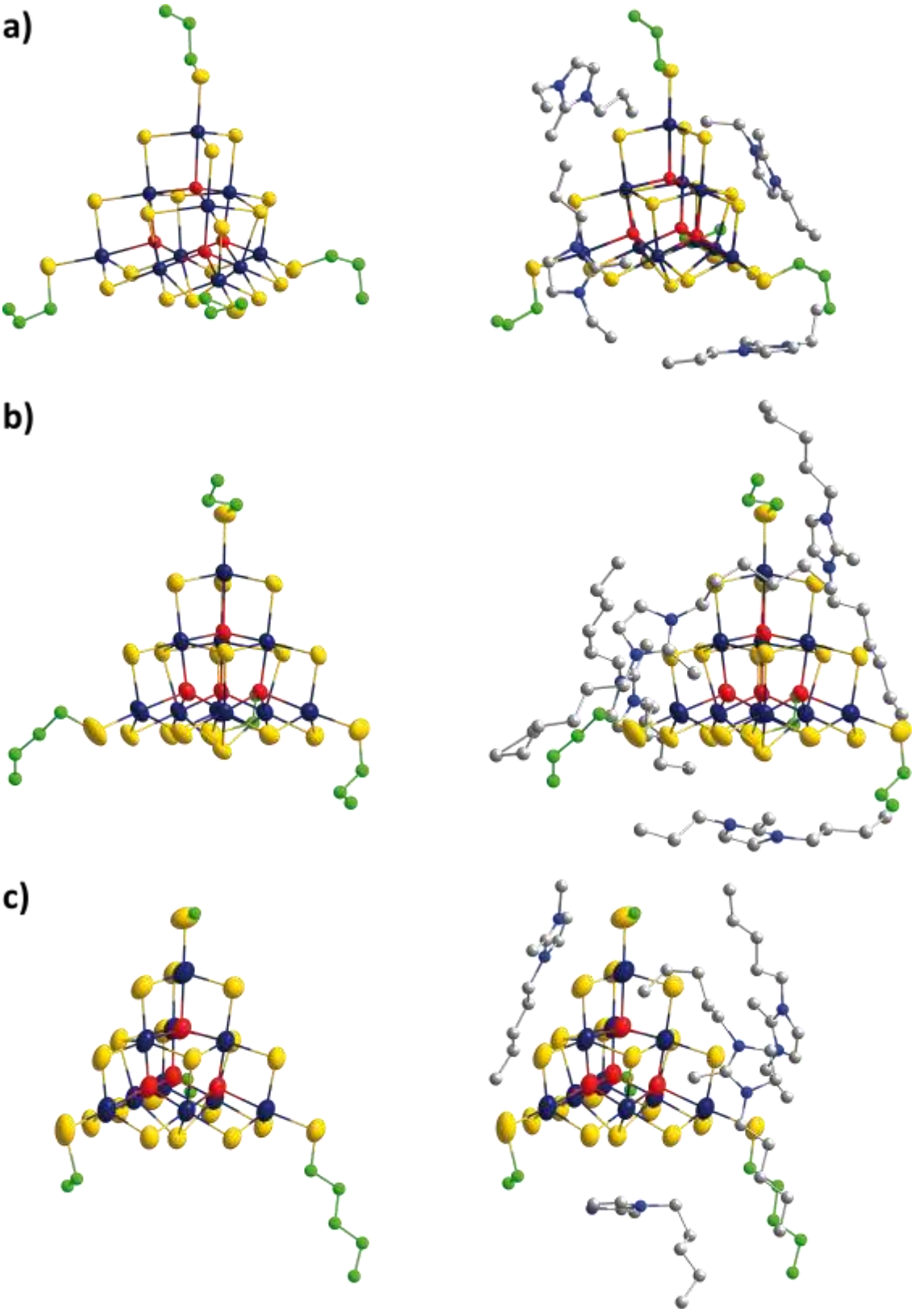

Figure S8. Illustration of the compounds a) **1**, b) **2** and c) **3**. The cluster anions of **1**, **2** and **3** (left). The cluster anions of **1**, **2** and **3** with the four closest ionic liquid cations (right). H-atoms are omitted for clarity. As rather typical for these compounds, not all C atoms of the alkyl groups could be located by the SCXRD analysis owing to the longer alkyl chains' high flexibility and disorder. Color code: Sn dark blue, O red, S yellow, C green and grey, N blue.

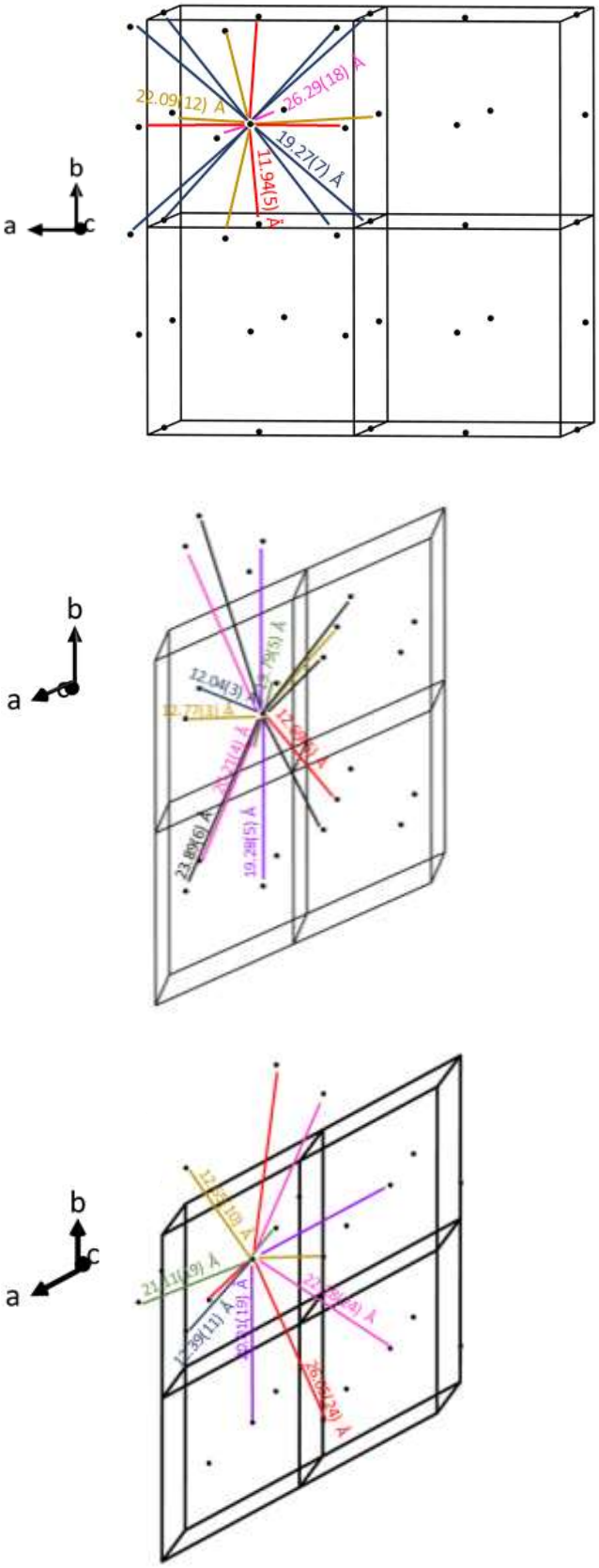

Figure S9. Illustration of the cluster center··· cluster center distances found in compounds **1** (top), **2** (center), and **3** (bottom). For this purpose, a dummy atom was placed in the center of the cluster core (shown as black spheres), and their distances were determined as shown. Crystallographically equivalent distances in one compound are illustrated in the same color

4.2 Details of Intrinsic Crystallographic Issues Concerning Compounds 2 and 3

Compound 2:

Main problem: Owing to high conformational freedom of the pentyl groups, the electron density of some of the C atoms is "smeared" in space in a way that makes it impossible to localize them on the difference Fourier map. For the same reason, some of the C atoms that can be localized still have a high displacement tendency, so they cannot be reasonably refined using anisotropic displacement parameters (without producing "npd", results), nor does modelling of disorder help in these cases to improve the *R* values or the reasonability of the model. Here, we outline what we did to optimize the crystallographic data and refinement:

X-ray measurement:

We tried several ways of setting up the X-ray diffraction measurement for crystals of compound **2**:

1. STOE StadiVari diffractometer, Cu-Kα radiation (λ = 1.54186 Å), immediate cooling from room temperature (r.t.) to 100 K upon mounting the crystal.

2. STOE StadiVari diffractometer, Cu-Kα radiation, slow cooling from r.t. to 100 K up-on mounting the crystal (10 K per hour)

3. Bruker Quest diffractometer, Mo-Kα radiation (λ = 0.71073 Å) radiation, immediate cooling from r.t. to 100 K upon mounting the crystal.

→ Measurement no. 1 produced the best data set.

Refinement:

Problem 1: We cannot refine all C atoms of the alkyl chains, although we tried the following variations:

1. Model disorder of the alkyl chains at once

→ The refinement did not converge with all-connected C atoms in the alkyl chains

2. Refine C atoms stepwise on single or disordered positions to "build up" the chains atom by atom

→ Works for some of the atoms, but not for the whole alkyl chains.

Problem 2: We cannot reasonably calculate H atoms to ride on the highly mobile C atoms. This applies especially to C atoms in 4-position of the chain if the atoms in 5-position are missing. We tried all variations of HFIX together with a diversity of further SHELX commands in Olex to cope with the "open" connectivity of the 5th C atoms, but none of these refinements converged into a reasonable set of C–H bonds. We are VERY experienced in the refinement of tricky crystal structures, but the data is limited owing to the intrinsic problem mentioned above.

Problem 3: In one of the imidazole rings, N atoms cannot be refined using anisotropic displacement parameters (hence, produces "npd" results), owing to the uncertainty of the C atoms attached. None of the known SHELX commands helps, so we decided to refine these atoms using isotropic displacement parameters, which is often found in the literature (in many cases also for entire organic groups).

Problem 4: Some of the C atoms have large displacement parameters, owing to the inherent mobility of the pentyl groups. However, they are still connected to the alkyl chains, so we consider this kind of modelling better than just deleting the respective atom from the atom list, which would also cause a correspondingly increased residual electron density peak.

Compound 3

Main problem: Owing to (even) high(er) conformational freedom of the hexyl groups, the electron density of some of the C atoms is "smeared" in space in a way that makes it impossible to localize them

on the difference Fourier map. For the same reason, some of the C atoms that can be localized still have a high displacement tendency, so they cannot be reasonably refined using anisotropic displacement parameters (without producing "npd", results), nor does modelling of disorder help in these cases to improve the *R* values or the reasonability of the model. Here, we outline what we did to optimize the crystallographic data and refinement:

X-ray measurement:

We tried several ways of setting up the X-ray diffraction measurement for crystals of compound **3**:

1. STOE StadiVari diffractometer, Cu-Kα radiation (λ = 1.54186 Å), immediate cooling from room temperature (r.t.) to 100 K upon mounting the crystal.

2. STOE StadiVari diffractometer, Cu-Kα radiation, slow cooling from r.t. to 100 K up-on mounting the crystal (10 K per hour)

3. Bruker Quest diffractometer, Mo-Kα radiation (λ = 0.71073 Å) radiation, immediate cooling from r.t. to 100 K upon mounting the crystal.

→ Measurement no. 1 produced the best data set.

Refinement:

Problem 1: We cannot refine all C atoms of the alkyl chains, although we tried the following variations:

1. Model disorder of the alkyl chains at once

→ The refinement did not converge with all-connected C atoms in the alkyl chains (except for two of the hexyl chains).

2. Refine C atoms stepwise on single or disordered positions to "build up" the chains atom by atom

→ Works for some of the atoms, but not for the whole alkyl chains.

Problem 2: We cannot reasonably calculate H atoms to ride on the highly mobile C atoms. This applies especially to C atoms in 4- or 5-position of the chain if the atoms in (5- and) 6-position are missing. We tried all variations of HFIX together with a diversity of further SHELX commands in Olex to cope with the "open" connectivity of the 5th C atoms, but none of these refinements converged into a reasonable set of C–H bonds. We are VERY experienced in the refinement of tricky crystal structures, but the data is limited owing to the intrinsic problem mentioned above.

Problem 3: Some of the C atoms have large displacement parameters, owing to the inherent mobility of the hexyl groups. However, they are still connected to the alkyl chains, so we consider this kind of modelling better than just deleting the respective atom from the atom list, which would also cause a correspondingly in-creased residual electron density peak. To cope with this problem, we needed to reduce the s.o.f. of some of the C atoms below 1.0. This makes full sense, as the partially occupied site is only one of several disorder positions of the respective atom, with the other ones being non-localizable in the smeared residual electron density.

In summary, the models we provide with our refinement of compounds **2** and 3 is the best we can get from crystals of this compound after numerous trials. We are convinced of the unambiguity of the chemical composition of our compound as it was confirmed by complementary analyses. The X-ray crystallography is another method to gain information of the cluster compound – and despite the described problems – offers the most precise information we can get about them.

We note in passing, that similar problems have been reported in many publications on compounds comprising cluster anions besides cations comprising organic groups.

5. Raman Spectroscopy

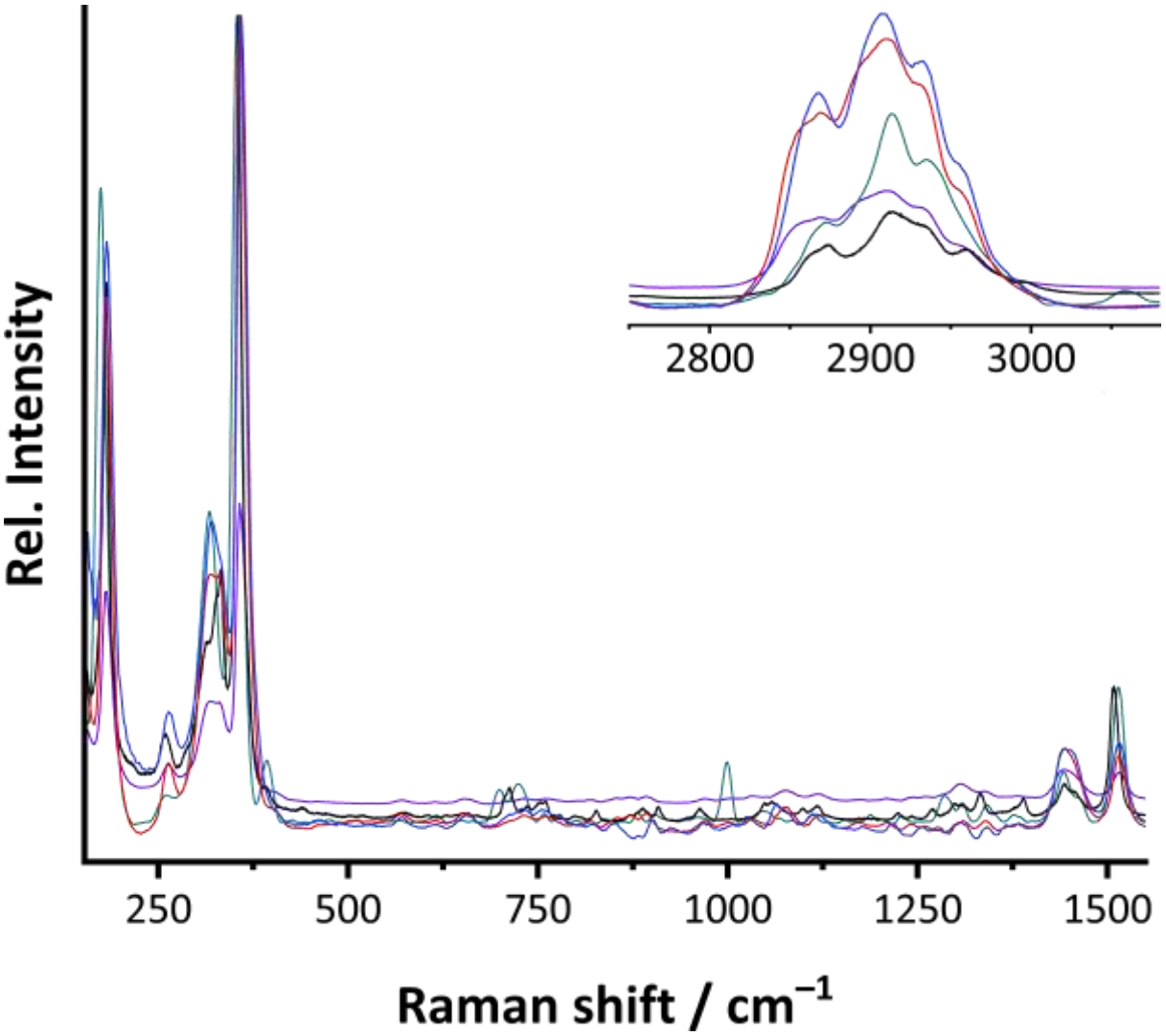

Figure S10. Raman spectra of **1** (black line), **2** (blue line), **3** (red line). Known spectra of the reported compounds $(C_4C_1C_1Im)_4[Sn_{10}O_4S_{16}(SMe)_4]$ (green line)[6] and $(C_4C_1C_4Im)_7[Sn_{10}O_4S_{16}(SBu)_4]Br_3$ (violet line)[7] are added for comparison.

The SC Raman spectra of **1**, **2**, and **3** (Figure S10) show the characteristic signal group of the inorganic framework between 100 and 400 cm^{-1}. The S–C vibrations that are indicative for the alkylation of the clusters are detected at ~735 to 760 cm^{-1}, with decreasing relative intensity for the clusters with longer alkyl chains. Characteristic bands of the C_{Alkyl}–H vibrations can be found at around 1500 cm^{-1}. The signal group of the imidazolium C_{Im}–H vibrations can be found at around 2900 cm^{-1}.

6. NMR Spectroscopy

6.1 ^{119}Sn NMR spectrum of a solution of 1 (with traces of attached reaction medium) in CH_3CN-d3.

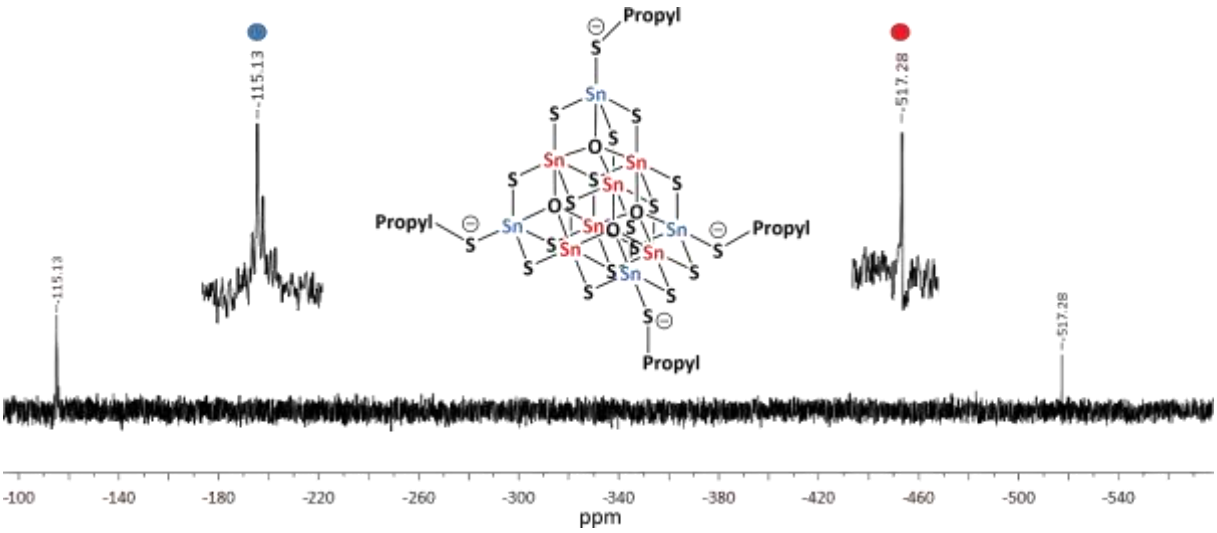

Figure S11. ^{119}Sn-NMR spectrum of a solution of **1** in CH_3CN-d3 with zoom into the signals assigned to the different Sn atomic sites.

6.2 ^{1}H NMR spectrum of a solution of 1 (with traces of attached reaction medium) in CH_3CN-d3.

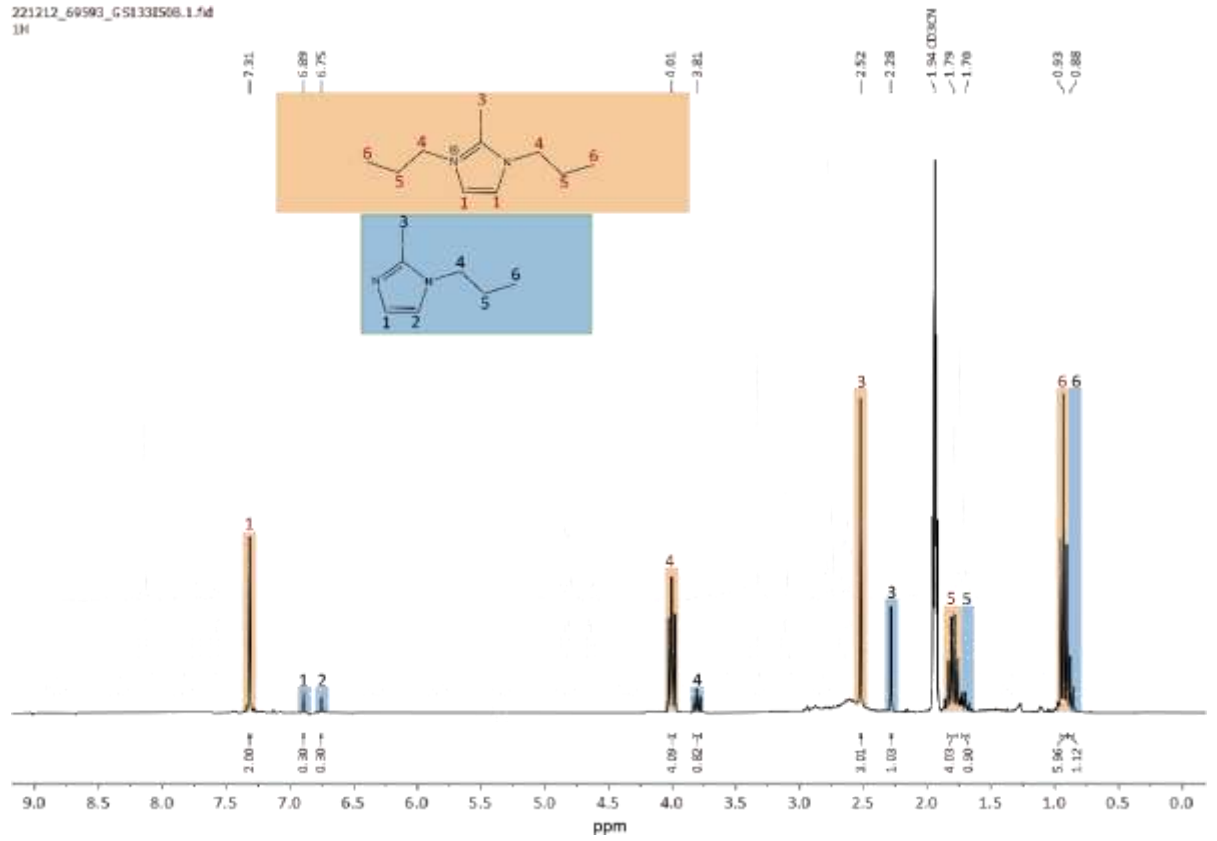

Figure S12.^{1}H-NMR spectrum of **1** in CH_3CN-d3.

The following signals can be assigned to ($C_3C_1C_3$Im)Br:

^{1}H-NMR (500.2 MHz, CD_3CN, 293 K): δ [ppm] = 7.31 (s, 2H, $C_{Im}H$); 4.01 (t, J = 7.5 Hz, 4H, CH_2); 2.52 (s, 3H, CH_3); 1.79 (m, 4H, CH_2); 0.93 (t, 6H, J = 7.3 Hz, CH_3)

The following signals can be assigned to (C_3C_1Im):

^{1}H-NMR (500.2 MHz, CD_3CN, 293 K): δ [ppm] = 6.89 (s, 1H, $C_{Im}H$); 6.75 (s, 1H, $C_{Im}H$); 3.81 (t, 2H, J = 7.1 Hz, CH_2); 2.28 (s, 3H, CH_3); 1.70 (m, 4H, CH_2); 0.88 (t, 3H, J = 7.4, CH_3)

6.3 ^{13}C NMR spectrum of a solution of 1 (with traces of attached reaction medium) in CH_3CN-d3.

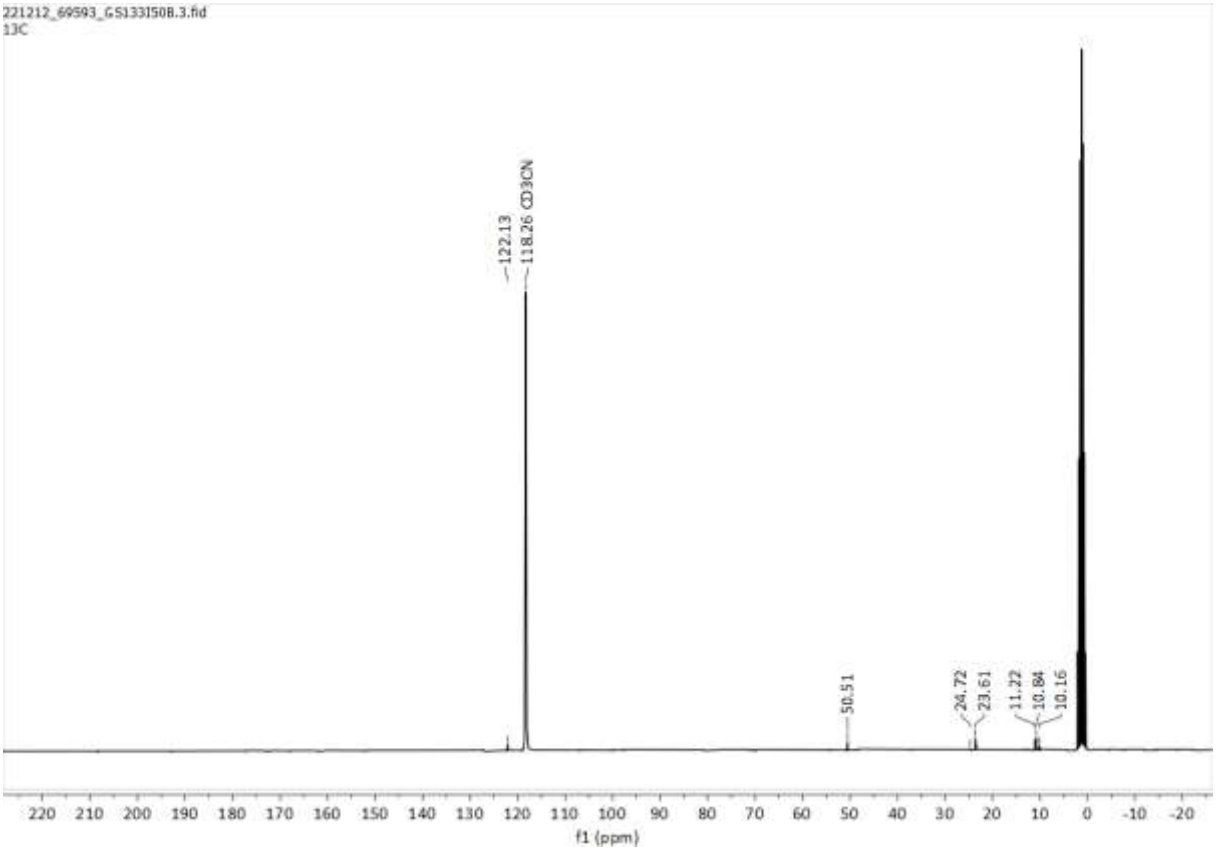

Figure S13. ^{13}C NMR spectrum of **1** in CH_3CN-d3.

The following signals can be assigned to ($C_3C_1C_3$Im)Br:

^{13}C-NMR (126 MHz, CD_3CN, 293 K) δ [ppm] = 122.75 (s, C_{Im}); 50.13 (s, CH_2); 23.23 (s, CH_3); 10.46 (s, CH_2); 9.78 (s, CH_3)

6.4 ^{119}Sn NMR spectrum of a solution of 2 (with traces of attached reaction medium) in CH3CN-d3

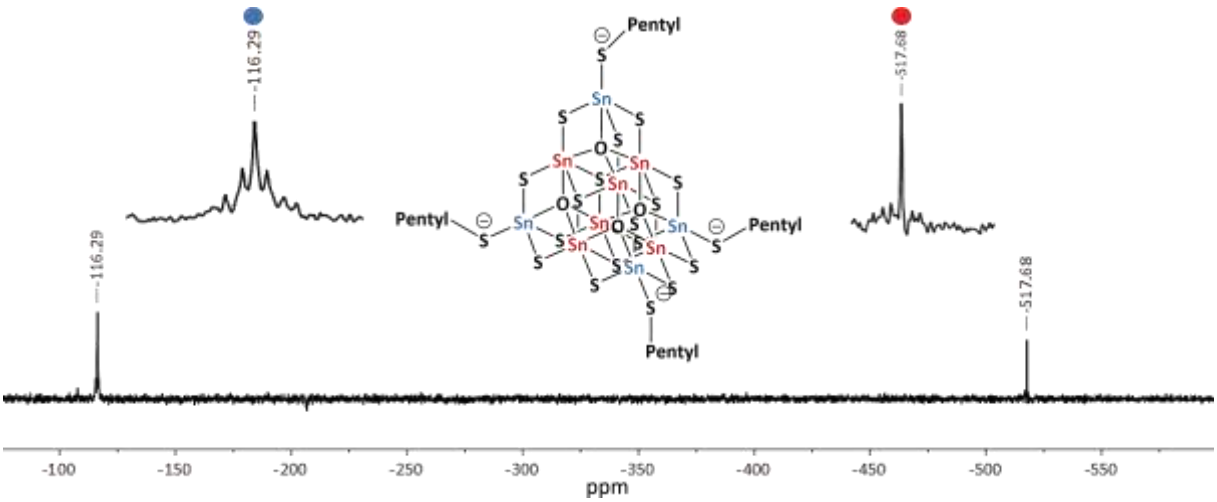

Figure S14. ^{119}Sn NMR spectrum of a solution of **2** in CH_3CN-d3 with zoom into the signals assigned to the different Sn atomic sites.

6.5 ^{1}H NMR spectrum of a solution of 2 (with traces of attached reaction medium) in CH_3CN-d3.

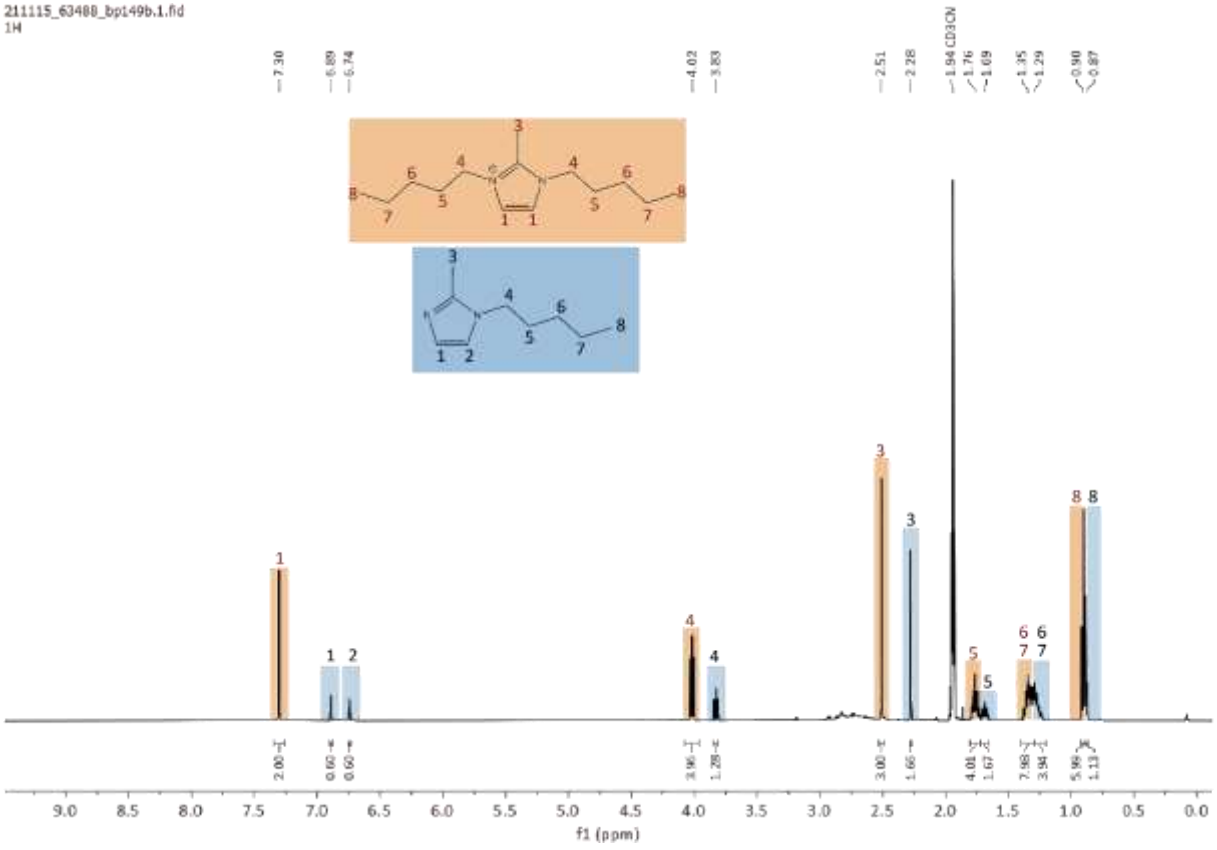

Figure S15.^{1}H-NMR spectrum of **2** in CH_3CN-d3.

The following signals can be assigned to ($C_5C_1C_5Im$)Br:

^{1}H-NMR (500.2 MHz, CD_3CN, 293 K): δ [ppm] = 7.3 (s, 2H, $C_{Im}H$); 4.02 (t, J = 7.7 Hz, 4H, CH2); 2.51 (s, 3H, CH_3); 1.76 (m, 4H, CH_2); 1.35 (m, 8H, CH_2); 0.90 (t, 6H, J = 7.1 Hz, CH_3)

The following signals can be assigned to (C_5C_1im):

^{1}H-NMR (500.2 MHz, CD_3CN, 293 K): δ [ppm] = 6.89 (s, 1H, $C_{Im}H$); 6.74 (s, 1H, $C_{Im}H$); 3.83 (t, 2H, J = 7.4 Hz, CH_2); 2.28 (s, 3H, CH_3); 1.69 (m, 4H, CH_2); 0.87 (t, 3H, J = 7.4, CH_3)

6.6 ^{13}C NMR spectrum of a solution of 2 (with traces of attached reaction medium) in CD_3CN.

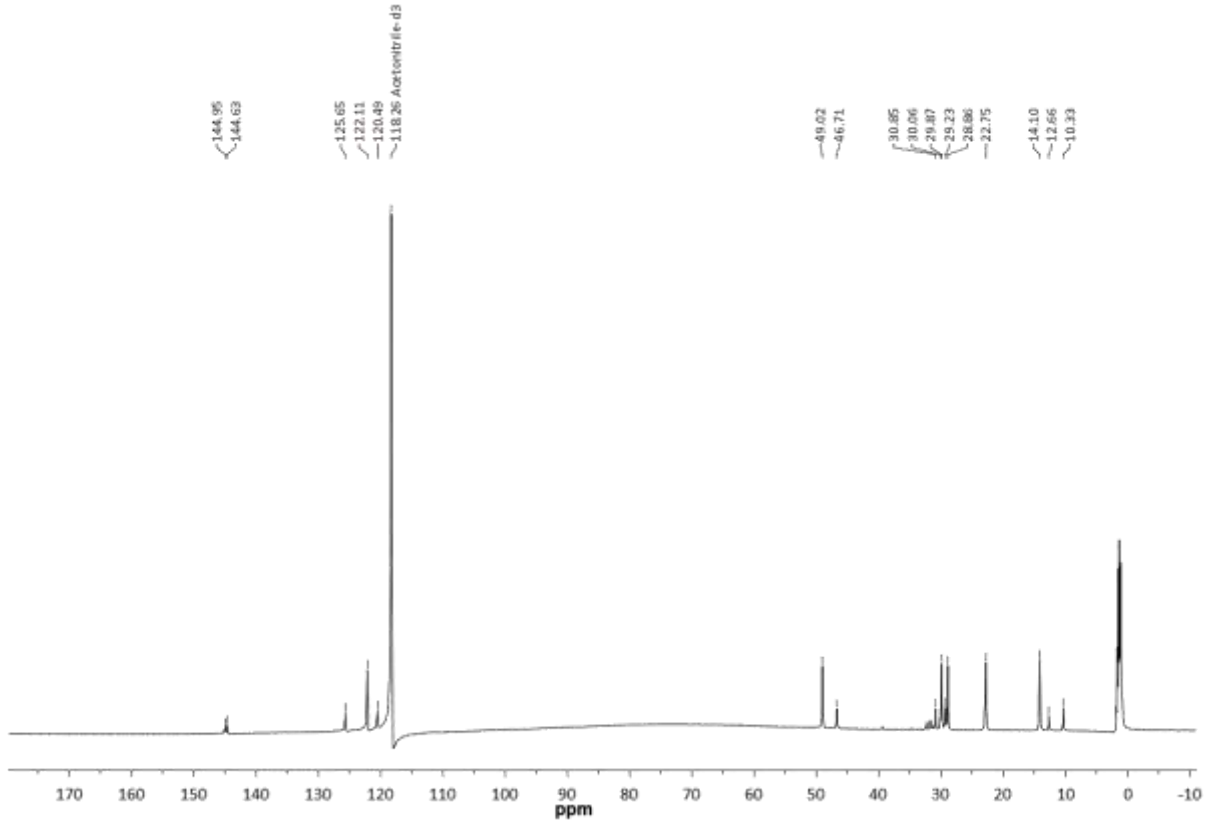

Figure S16. ^{13}C NMR spectrum of **2** in CH_3CN-d3.

The following signals can be assigned to ($C_5C_1C_5Im$)Br:

^{13}C-NMR (126 MHz, CD_3CN, 293 K) δ [ppm] = 144.63 (s, $C_{Im}Me$); 122.11 (s, C_{Im}); 49.02 (s, CH_2); 29.87 (s, CH_3); 28.86 (s, CH_2); 22.75 (s, CH_2); 14.10 (s, CH_2); 10.33 (s, CH_3)

The following signals can be assigned to (C_5C_1im):

^{13}C-NMR (126 MHz, CD_3CN, 293 K) δ [ppm] = 144.95 (s, $C_{Im}Me$); 125.65 (s, C_{Im}); 120.49 (s, C_{Im}); 46.71 (s, CH_2); 30.85 (s, CH_3); 30.06 (s, CH_2); 29.23 (s, CH_2); 12.66 (s, CH_3)

6.7 ^{119}Sn NMR spectrum of a solution of 1 (with traces of attached reaction medium) in CH_3CN-d3.

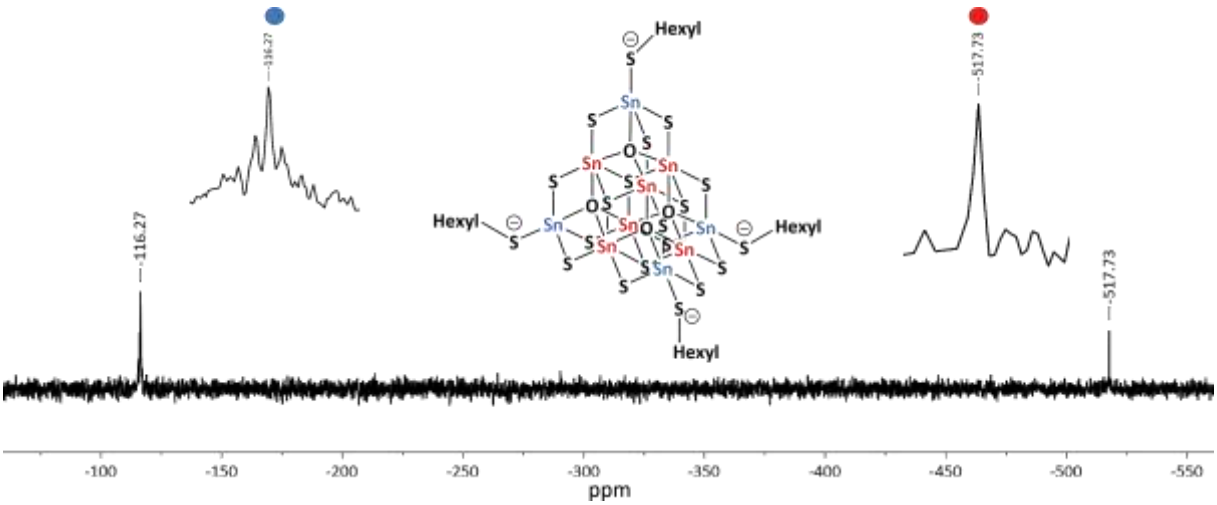

Figure S17. ^{119}Sn-NMR spectrum of a solution of **3** in CH_3CN-d3 with zoom into the signals assigned to the different Sn atomic sites.

6.8 ^{1}H NMR spectrum of a solution of 3 (with traces of attached reaction medium) in CD_3CN.

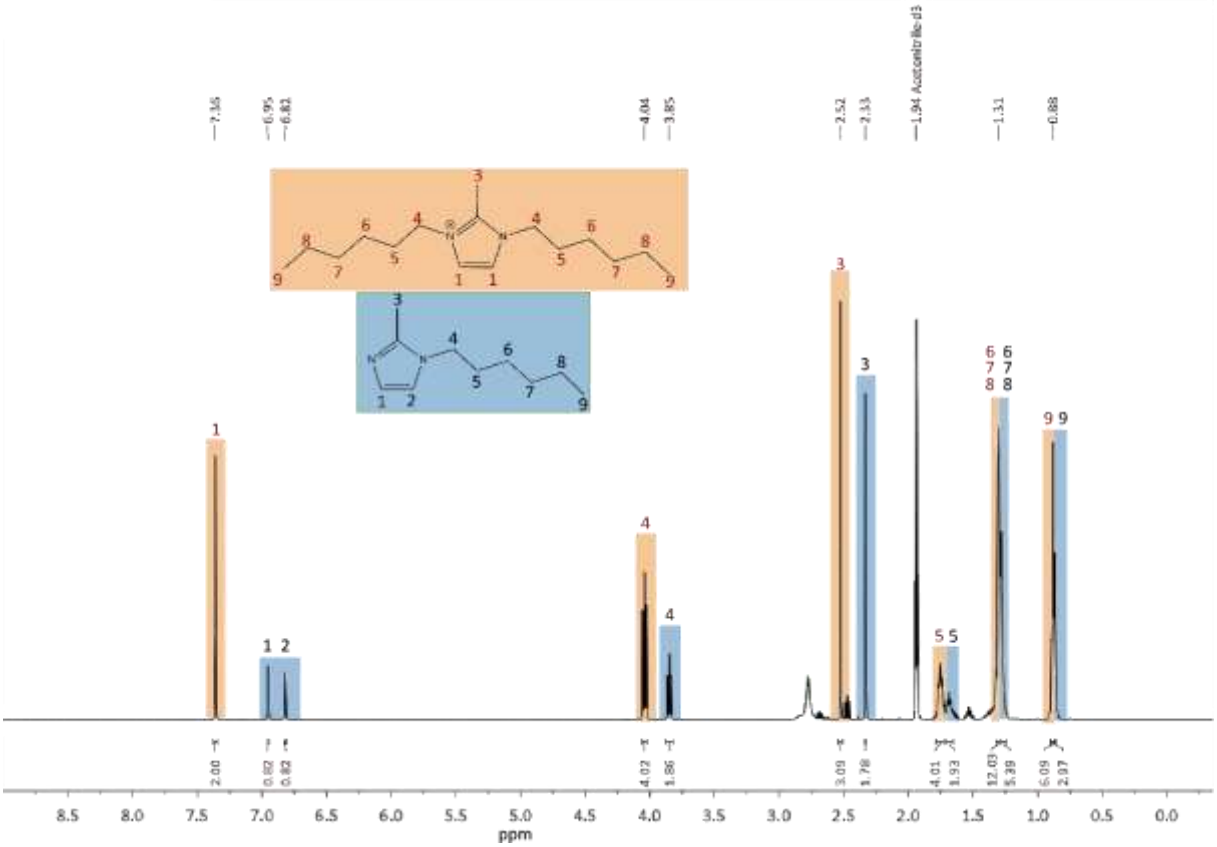

Figure S18.^{1}H-NMR spectrum of **3** in CH_3CN-d3.

The following signals can be assigned to ($C_6C_1C_6$Im)Br:

^{1}H-NMR (500.2 MHz, CD_3CN, 293 K): δ [ppm] = 7.36 (s, 2H, $C_{Im}H$); 4.04 (t, J = 7.3 Hz, 4H, CH_2); 2.52 (s, 3H, CH_3); 1.76 (m, 4H, CH_2); 1.31 (m, 12H, CH_2); 0.88 (m, 6H, J = 7.1 Hz, CH_3)

The following signals can be assigned to (C_6C_1im):

^{1}H-NMR (500.2 MHz, CD_3CN, 293 K): δ [ppm] = 6.95 (s, 1H, $C_{Im}H$); 6.82 (s, 1H, $C_{Im}H$); 3.85 (t, 2H, J = 7.3 Hz, CH_2), 2.33 (s, 3H, CH_3); 1.28 (m, 6H, CH_2); 0.86 (m, 3H, J = 6.8 Hz, CH_3)

6.9 ^{13}C NMR spectrum of a solution of 3 (with traces of attached reaction medium) in CD_3CN.

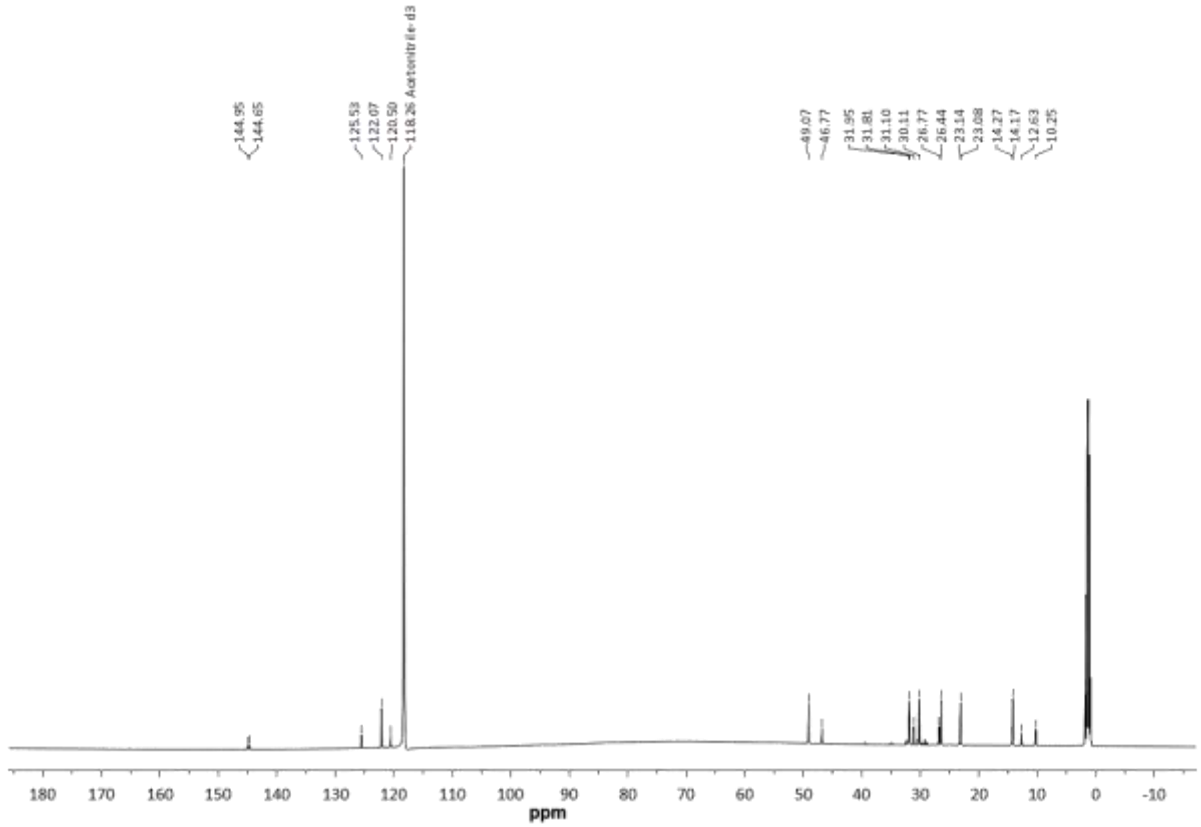

Figure S19. ^{13}C-NMR spectrum of **3** in CH_3CN-d3.

The following signals can be assigned to ($C_6C_1C_6$Im)Br:

^{13}C-NMR (126 MHz, CD_3CN, 293 K) δ [ppm] = 144.65 (s, $C_{Im}Me$); 122.07 (s, C_{Im}); 49.07 (s, CH_2); 31.81 (s, CH_3); 30.11 (s, CH_2); 26.44 (s, CH_2); 23.08 (s, CH_2); 14.17 (s, CH_2), 10.25 (s, CH_3)

The following signals can be assigned to (C_6C_1im):

^{13}C-NMR (126 MHz, CD_3CN, 293 K) δ [ppm] = 144.95 (s, $C_{Im}Me$); 125.53 (s, C_{Im}); 120.50 (s, C_{Im}); 46.77 (s, CH_2); 31.91 (s, CH_3); 31.10 (s, CH_2); 26.77 (s, CH_2); 23.14 (s, CH_2); 14.27 (s, CH_2); 12.63 (s, CH_3)

7. Electrospray Ionization Mass Spectrometry (ESI-MS)

5.1 ESI(–) Mass Spectra of Compound 1

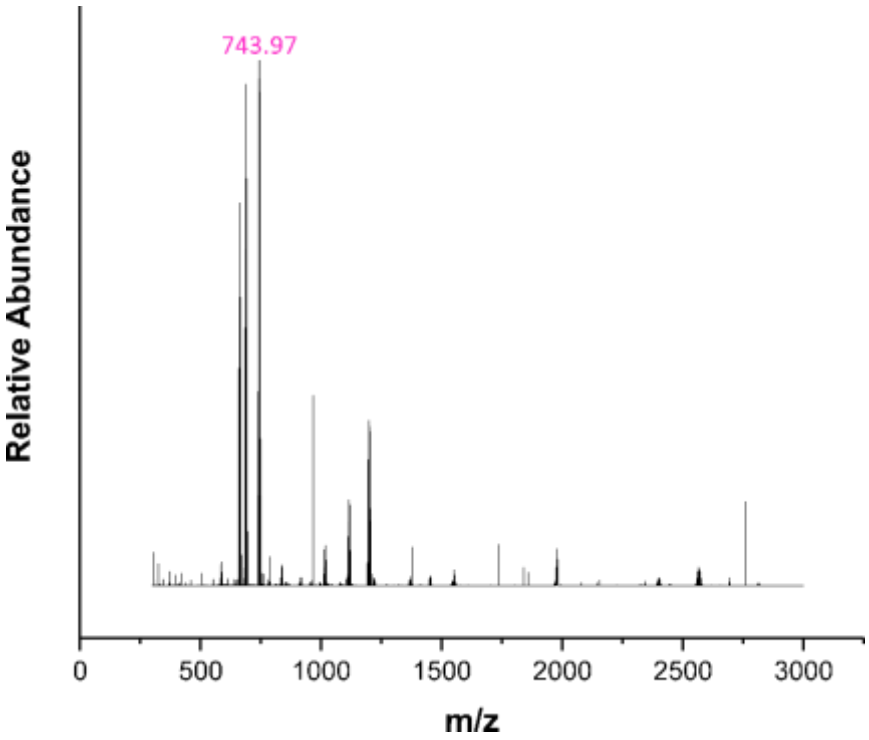

Figure S20. Overview of the ESI(–) mass spectrum of a fresh solution of single crystals of compound **1** in CH_3CN.

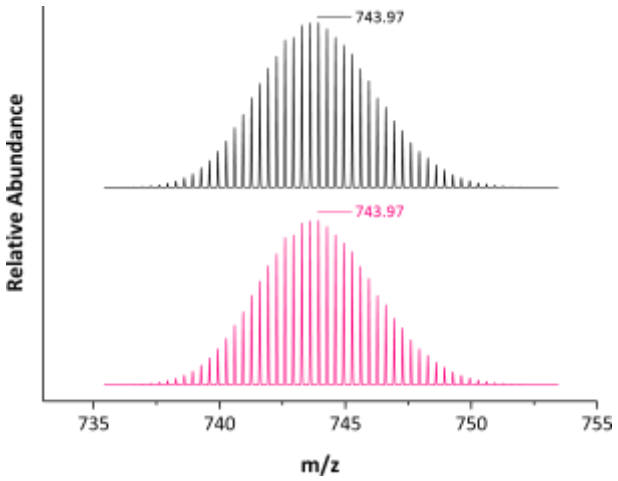

Figure S21. High-resolution mass peak of the cluster anion of **1**, detected as an aggregate of the anion with one ionic liquid counterion yielding a 3– charge. Top: simulated, bottom: measured.

5.2 ESI(–) Mass Spectra of Compound 2

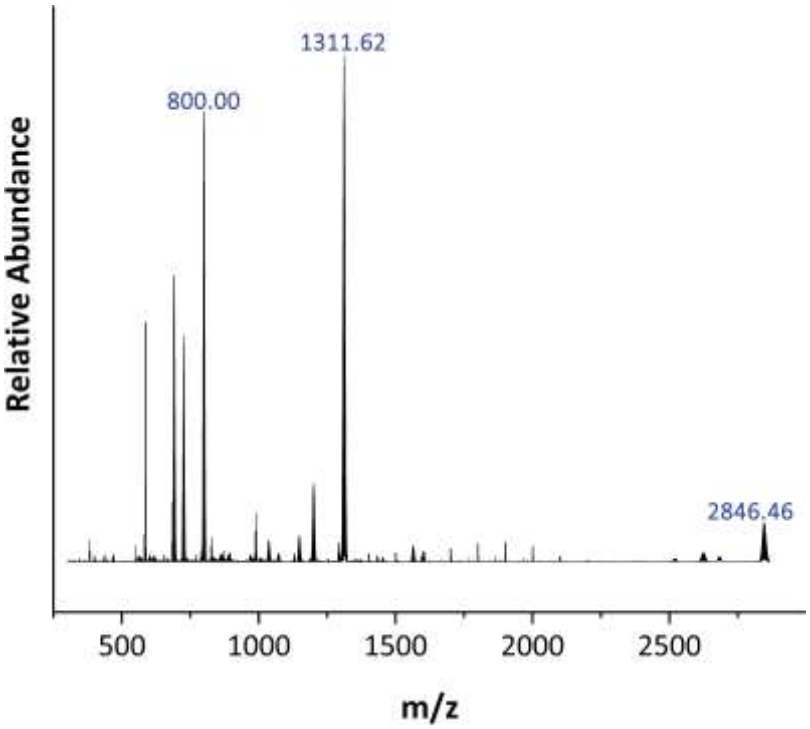

Figure S22. Overview of the ESI(–) mass spectrum of a fresh solution of single crystals of compound **2** in CH_3CN. Signals without labels refer to fragments that could not be unambiguously identified.

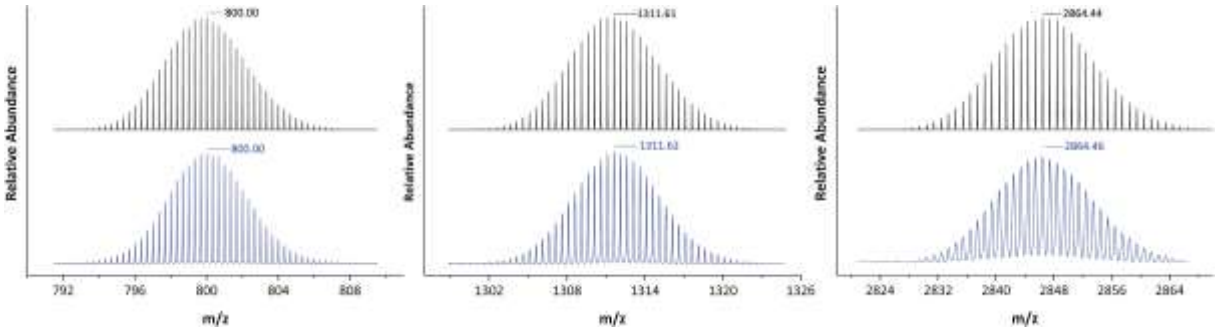

Figure S23. High-resolution mass peaks of the cluster anion of **2**, detected as an aggregate of the anion with one ionic liquid counterion yielding a 3– charge (a), with two ionic liquid counterions yielding a 2– charge (b), and with three ionic liquid counterions yielding a 1– charge (c). Top: simulated, bottom: measured.

5.3 ESI(–) Mass Spectra of Compound 3

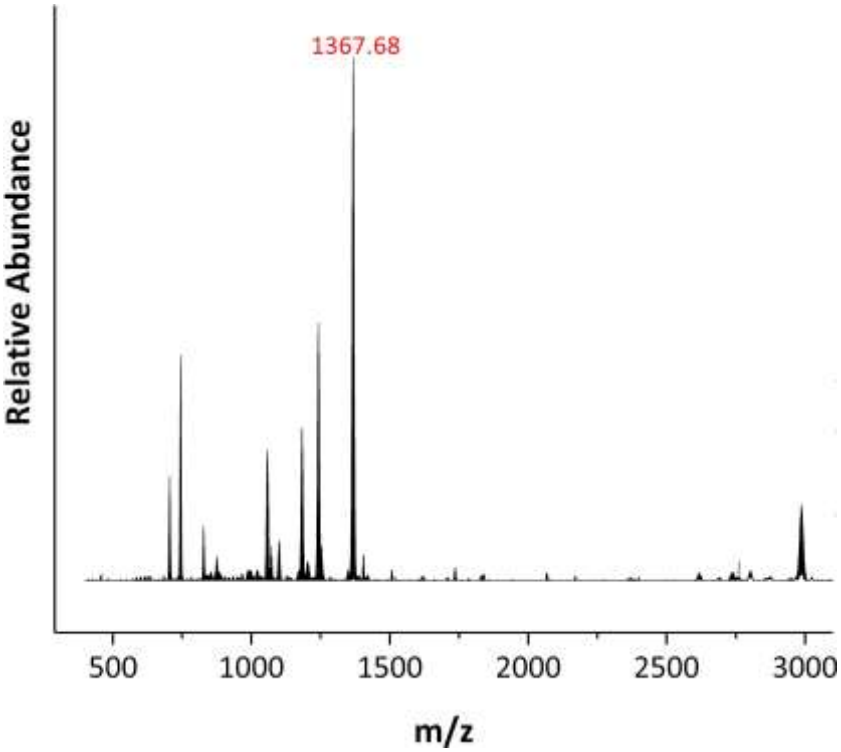

Figure S24. Overview of the ESI(–) mass spectrum of a fresh solution of single crystals of compound **3** in CH_3CN. Only one of the peaks could be assigned to a reasonable formula, while the other signals refer to fragments that could not be unambiguously identified.

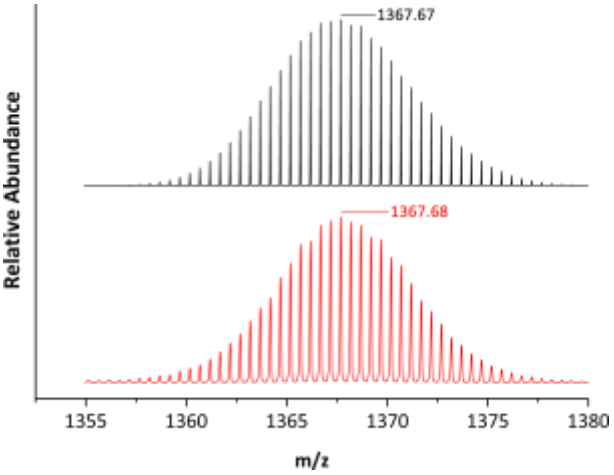

Figure S25. High-resolution mass peaks of the cluster anion of **3**, detected as an aggregate of the anion with two ionic liquid counterions yielding a 2– charge. Top: simulated, bottom: measured.

8. Optical Absorption Spectroscopy

8.1 Optical absorption spectra and Tauc plots of single crystals of 1.

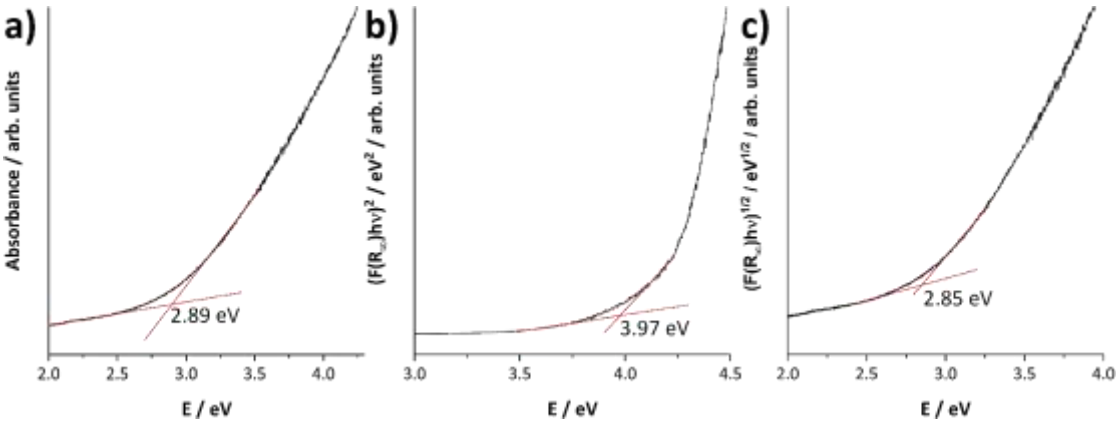

Figure S26. a) UV-visible absorbance spectra of single crystals of **1**, b) Tauc plots generated using the Kubelka-Munk-function $(F(R_\infty)h\nu)^{1/\gamma}$ with $\gamma = 0.5$ and c) $\gamma = 2$ of **1**.

8.2 Optical absorption spectra and Tauc plots of single crystals of 2.

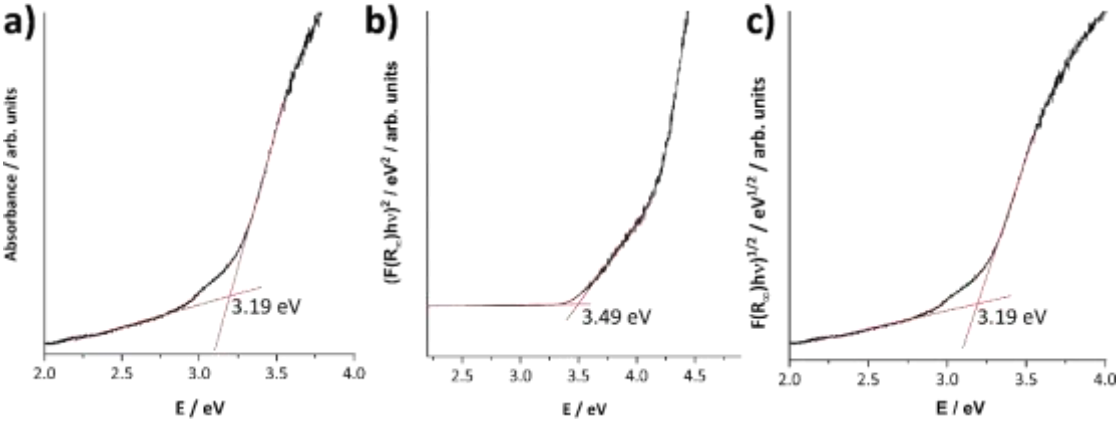

Figure S27. a) UV-visible absorbance spectra of single crystals of **2**, b) Tauc plots generated using the Kubelka-Munk-function $(F(R_\infty)h\nu)^{1/\gamma}$ with $\gamma = 0.5$ and c) $\gamma = 2$ of **2**.

8.3 Optical absorption spectra and Tauc plots of single crystals of 3.

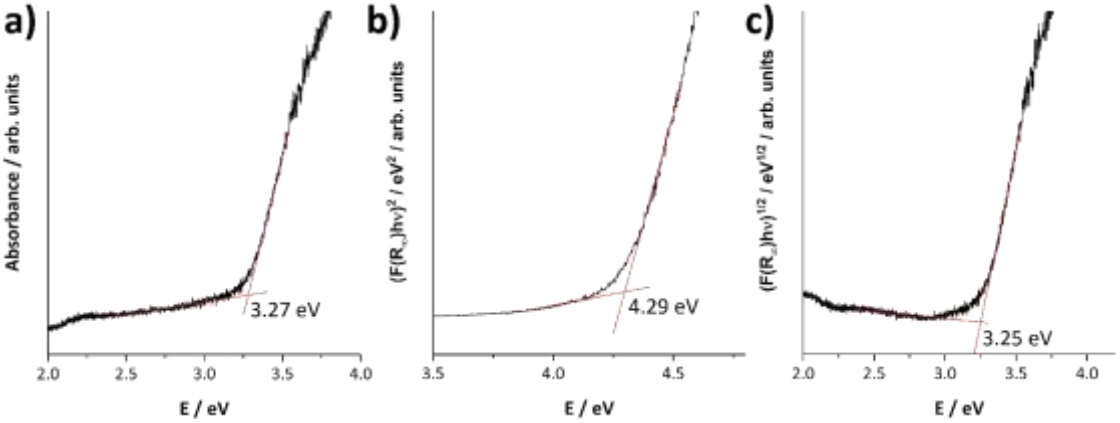

Figure S28. a) UV-visible absorbance spectra of single crystals of **3**, b) Tauc plots generated using the Kubelka-Munk-function $(F(R_\infty)h\nu)^{1/\gamma}$ with $\gamma = 0.5$ and c) $\gamma = 2$ of **3**.

9. Photoluminescence Spectroscopy

9.1 Photoluminescence spectra of 1, 2 and 3

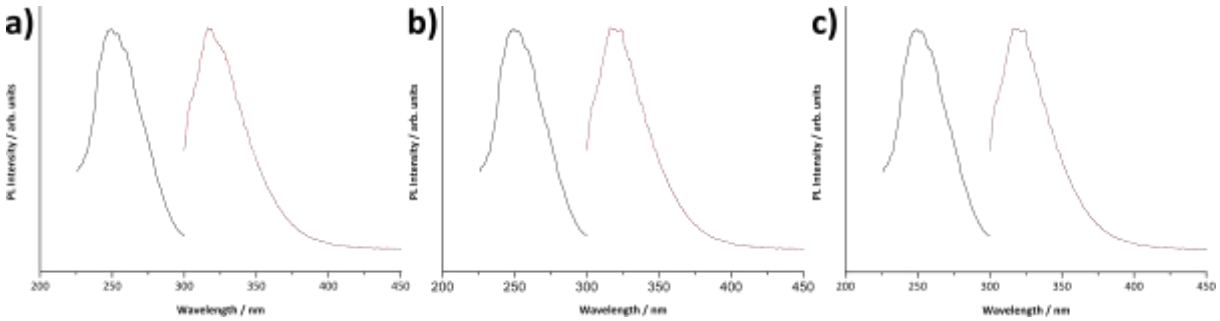

Figure S29. Photoluminescence properties of a) **1** (excitation: black line, λ_{ex} = 249 nm, emission: red line, λ_{em} = 317 nm), b) **2** (excitation: black line, λ_{ex} = 249 nm; emission: red line, λ_{em} = 317 nm), **3** (excitation: black line, λ_{ex} = 249 nm; emission: red line, λ_{em} = 317 nm). All measurements were recorded in CH_3CN solution.

9.2. Photoluminescence spectra of ionic liquids

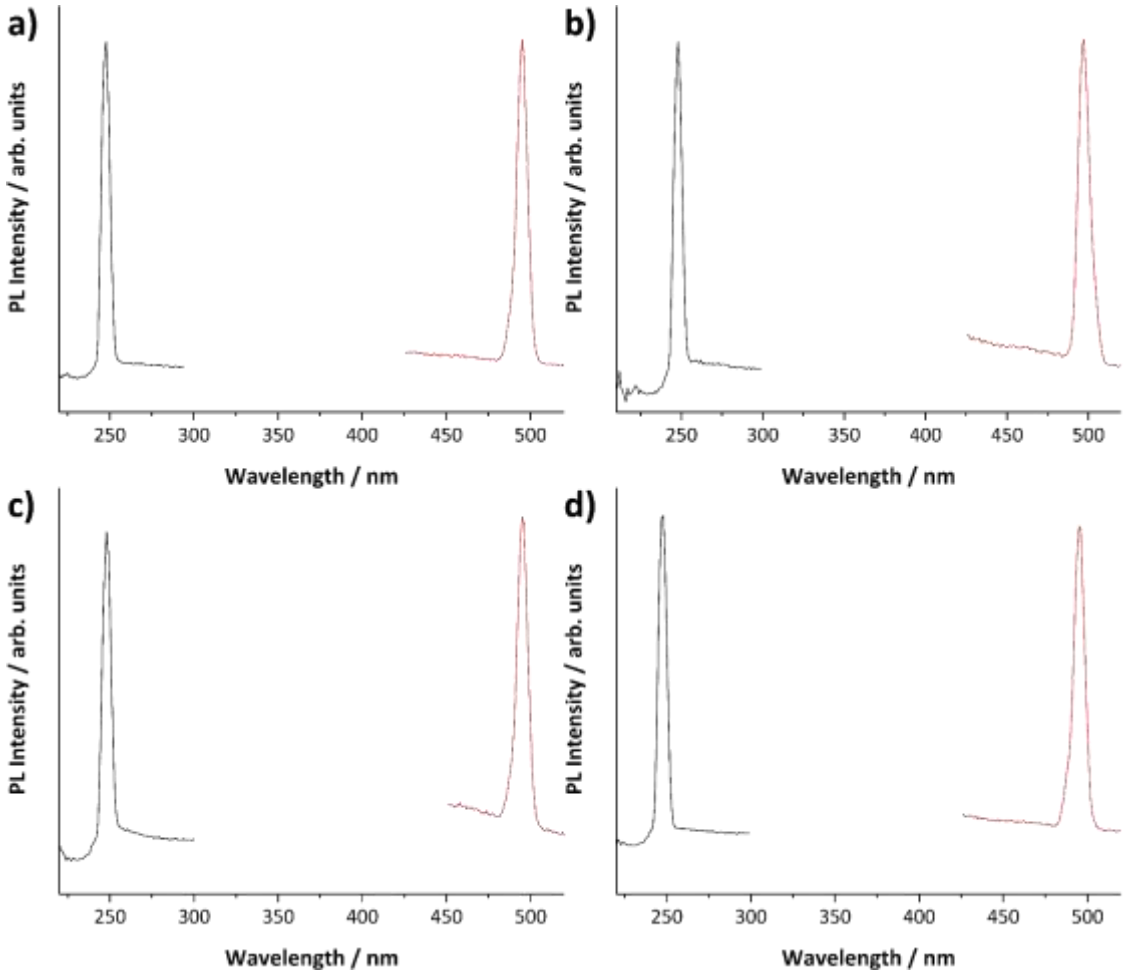

Figure S30. Photoluminescence properties of a) $(C_3C_1C_3Im)Br$ (excitation: black line, λ_{ex} = 247 nm; emission: red line, λ_{em} = 494 nm), b) $(C_5C_1C_5Im)Br$ (excitation: black line, λ_{ex} = 247 nm; emission: red line, λ_{em} = 494 nm), c) $(C_5C_1C_5Im)Br$ (excitation: black line, λ_{ex} = 247 nm; emission: red line, λ_{em} = 494 nm), d) $(C_6C_1C_6Im)Br$ (excitation: black line, λ_{ex} = 247 nm; emission: red line, λ_{em} = 494 nm). All measurements were recorded in CH_3CN solution.

10. References for the Supporting Information

1 W. Schiwy, S. Pohl and B. Krebs, *Z. Anorg. Allg. Chem.*, 1973, **402**, 77–86.
2 K. Boruah and R. Borah, *ChemistrySelect*, 2019, **4**, 3479–3485.
3 G. M. Sheldrick, *Acta Crystallogr C Struct Chem*, 2015, **71**, 3–8.
4 G. M. Sheldrick, *Acta Crystallogr A Found Adv*, 2015, **71**, 3–8.
5 O. V. Dolomanov, L. J. Bourhis, R. J. Gildea, J. A. K. Howard and H. Puschmann, *J Appl Crystallogr*, 2009, **42**, 339–341.
6 B. Peters, S. Santner, C. Donsbach, P. Vöpel, B. Smarsly and S. Dehnen, *Chem. Sci.*, 2019, **10**, 5211–5217.
7 B. Peters, G. Stuhrmann, F. Mack, F. Weigend and S. Dehnen, *Angew. Chem. Int. Ed.*, 2021, **60**, 17622–17628.
8 A. Murphy, *Solar Energy Materials and Solar Cells*, 2007, **91**, 1326–1337.
9 P. Kubelka and F. Munk, *Z. Techn. Phys.*, 1931, 593–601.
10 P. Makuła, M. Pacia and W. Macyk, *J. Phys. Chem. Lett.*, 2018, **9**, 6814–6817.
11 K. A. Michalow, D. Logvinovich, A. Weidenkaff, M. Amberg, G. Fortunato, A. Heel, T. Graule and M. Rekas, *Catalysis Today*, 2009, **144**, 7–12.